Zeitschrift: Eclogae Geologicae Helvetiae
Herausgeber: Schweizerische Geologische Gesellschaft
Band: 95 (2002)
Heft: 2

Artikel: Structural features of south-western Sardinian shelf (Western Mediterranean) deduced from aeromagnetic and high-resolution reflection seismic data
Autor: Fais, Silvana / Klingele, Emil E. / Lecca, Luciano
DOI: https://doi.org/10.5169/seals-168953

0012-9402/02/020169-14
Birkhäuser Verlag, Basel, 2002

Eclogae geol. Helv. 95 (2002) 169–182

Structural features of south-western Sardinian shelf (Western Mediterranean) deduced from aeromagnetic and high-resolution reflection seismic data

SILVANA FAIS[1], EMIL E. KLINGELÉ[2] & LUCIANO LECCA[3]

Key words: SW Sardinian shelf, Miocene, aeromagnetic, reflection seismics, interpretation.

ABSTRACT

This paper presents the continuation of an integrated geophysical and geological study of the continental shelf of western Sardinia in its southern part. The study wich was conducted because of the presence of a set of very strong elongated magnetic anomalies that have never been quantitatively interpreted, consists of an integrated interpretation of high-resolution reflection seismic and magnetic data. Thanks to Sparker high-resolution seismic data interpretation, it was possible to reconstruct the main structural features of the upper part of the south-western continental margin.

In the geological and structural contexts of the studied area, the aeromagnetic data was interpreted by a combination of two-dimensional Werner and Euler deconvolutions and by a delineation technique based on the maxima of the radial horizontal derivative, which proved to be very effective. The results of these techniques combined with those of high-resolution reflection seismics were used as constraints for a three-dimensional magnetic modelling. Thanks to the study, which was carried out in the laboratory on rock samples from the most representative lithotypes outcropping on land, and to the application of a special processing on pole reduced data, it was possible to ignore the effect of remanent magnetisation.

From the geological meaning of the 3D magnetic interpretation it was possible to improve our knowledge of the structure of the upper part of the continental margin and of new elements in volcano-tectonic evolution. In particular it was evidenced the presence of crustal faults that caused the lowering of the blocks of the south-western continental margin. The extensional tectonics that produced the block faulting also produced andesitic and ignimbritic volcanism during the Lower and Middle Miocene time span.

RIASSUNTO

Questo lavoro presenta uno studio integrato, geofisico e geologico, sulla piattaforma continentale della Sardegna sud-occidentale. Lo studio, realizzato mediante l'interpretazione integrata di dati sismici a riflessione ad alta risoluzione e di dati magnetici, è stato attuato allo scopo di definire le cause di una serie di anomalie magnetiche di particolare intensità finora non interpretate quantitativamente. I principali lineamenti tettonici della parte superiore del margine continentale sud-occidentale sono stati definiti mediante l'interpretazione dei dati sismici Sparker. I dati aeromagnetici sono stati interpretati mediante una combinazione delle tecniche di deconvoluzione di Werner ed Eulero e mediante il calcolo dei massimi delle derivate orizzontali del campo totale. I risultati ottenuti con l'applicazione di queste tecniche, integrati con quelli ottenuti dai dati sismici, hanno costituito i vincoli per il successivo *modelling* tridimensionale. L'effetto della magnetizzazione rimanente è risultato trascurabile a seguito di uno studio su campioni dei litotipi più rappresentativi, affioranti nelle vicine aree emerse, e dell'applicazione di un trattamento basato sulla riduzione al polo. L'interpretazione geologica del *modelling* tridimensionale ha consentito di migliorare le conoscenze sulla struttura del margine continentale superiore e sulla sua evoluzione tettono-vulcanica. In particolare, si è dedotta la presenza di faglie crostali che hanno causato l'abbassamento dei blocchi di questo settore di margine e hanno dato origine al vulcanismo andesitico ed ignimbritico durante il Miocene inferiore e medio.

Introduction

The offshore zone of south-western Sardinia shows a particularly intriguing magnetic pattern which is made up of a set of strong magnetic anomalies with amplitudes larger than 500 nT (anomaly A in Fig. 1), extending for approximately 15 km with a width of about 5 km. It is oriented NW-SE and is made up of a prominent elongated anomaly bounded to the north by two almost circular positive anomalies of an amplitude of 200 nT (anomalies B and C in Fig. 1). The first analyses on these anomalies were carried out by Cassano et al. (1979) and Cassano (1990), though no quantitative interpretation had ever been advanced so far. Recently, a geological-geophysical interpretation on the middle sector of this shelf and a general interpretation of magnetic anomalies of the western Mediterranean have been presented (Fais et al. 1996; Zanolla et al. 1998).

[1] Dipartimento di Geoingegneria e Tecnologie Ambientali, Piazza d'Armi, I-09123, Cagliari, Italy. E-mail: sfais@unica.it
[2] Geodesy and Geodynamics Laboratory, IGP, ETH Hönggerberg, CH-8093 Zurich, Switzerland. E-mail: klingele@geod.baug.ethz.ch
[3] Dipartimento di Scienze della Terra, Via Trentino 51, I-09127, Cagliari, Italy. E-mail: leccal@unica.it

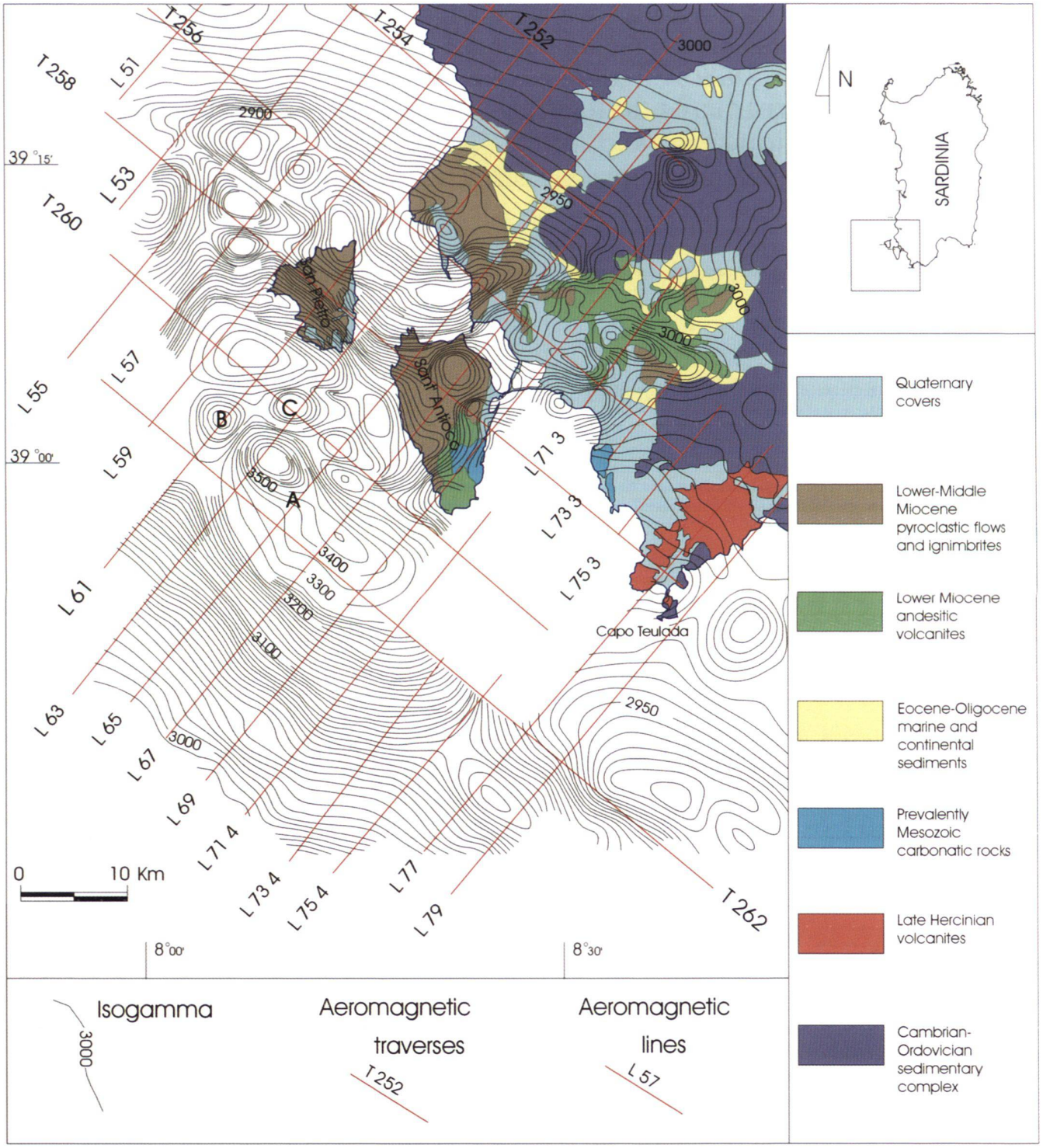

Fig. 1. Geological sketch of the studied area with location of the flight lines of the aeromagnetic survey and resulting magnetic residual anomalies.

The aim of this paper is to propose a three-dimensional magnetic model that can explain the origin of these anomalies. To this purpose we tried to produce a consistent synthesis of the results of two and three-dimensional magnetic deconvolutions, a three-dimensional magnetic modelling, and the interpretation of high-resolution reflection seismics.

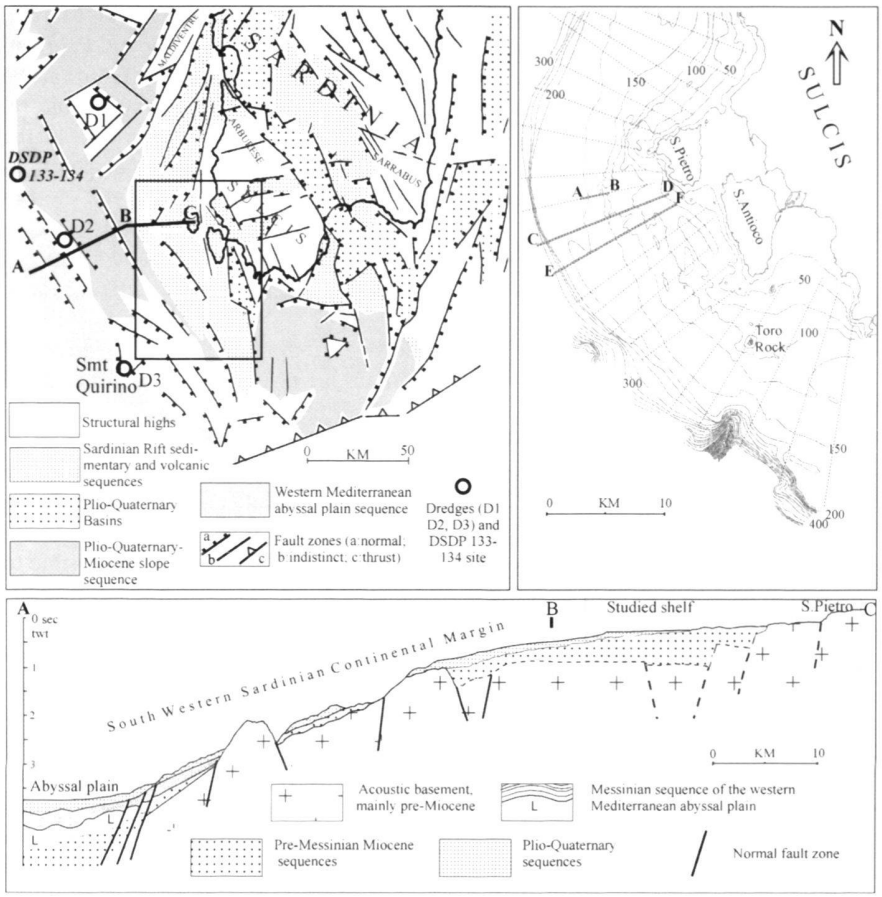

Fig. 2. Upper left: location of the studied area on the frame of the structural sketch of south Sardinia. Upper right: bathymetry of the studied area with location of analysed seismic reflection profiles (dotted lines), A-B, C-D and E-F locations of the cross sections of figures 3 and 4 respectively. Below: schematic cross-section of the south-western Sardinian continental margin, based on 10 cubic inch air gun (A-B) and 1kJ sparker (B-C) seismic reflection profiles, see upper left for location.

The presence of these anomalies in the upper part of the continental margin of south-western Sardinia and their quantitative interpretation give a better account of the structural and evolutionary elements of this sector.

Geological setting

The diverging continental margin of western Sardinia originated during the opening of the western Mediterranean in Oligo-Miocene times, as a back arc basin relating to the subduction towards north-west of a remnant Mesozoic oceanic crust (Finetti & Morelli 1973; Biju Duval & Montadert 1977; Rehault et al. 1985; Dewey et al. 1989). This back arc basin probably developed above a branch of the Pyrenean orogeny (Fanucci & Morelli 1995), therefore the presence of folds, reverse faults, and tectono-sedimentary units in south-western Sardinia on Mesozoic and Palaeogenic outcrops (Barca & Costamagna 2000) could be interpreted in this sense.

The tectonic structures of this margin are linked to those of the Sardinian Rift (Fig. 2-upper left), which is also of Oligo-Miocene age (Cherchi & Montadert 1982), and makes up a transtensional-extensional system propagating within an eastward migrating Sardinia-Corsica micro-plate (Lecca et al. 1997).

This margin is structured on the Palaeozoic basement and reactivated Hercynian structures. Consequently, the rocks that make up the margin are prevalently metamorphic Hercynian schists and granitoids, locally covered both by Mesozoic-Tertiary terrigenous and carbonate sequences and by calcalkaline volcanic sequences effused during the Oligo-Miocene rifting.

The phases of the rifting caused the emplacement of andesitic volcanic complexes both at the regional scale, in a peripheral position with respect the Sulcis-Arburese tectonic horst block complex, and at the scale of the Sulcis block within transversal grabens. In particular, the Sulcis and the S.Antioco-S.Pietro area were affected by an extensional fault system that crossed the crust and gave rise to several volcanic foci, both in the Oligo-Miocene and in the lower-middle-Miocene. Therefore a number of effusive and explosive volcanic complexes outcrop in the island of Sant'Antioco and San Pietro (Garbarino et al. 1985; Maccioni et al. 1990), and along the transversal graben of western Sulcis. Within this graben, the volcanic complexes (Assorgia et al. 1992; Brotzu et al. 1997) crossed and covered the M. Margiani sandstones of the Late Palaeocene-early Eocene (Barca & Costamagna 2000), the lignitiferous sequence (Ilerdian and Cuisian; Barberi & Cherchi 1980; Matteucci 1985), the overlying fluvial complexes of the

Cixerri Formation (Late Eocene-Early Oligocene) and locally an alluvial complex correlated with the Ussana Formation (late Oligocene-early Miocene) of Pecorini & Pomesano-Cherchi (1969).

Looking at the oldest andesites of the Sulcis graben, the ages are close to about 28 Ma (Brotzu et al. 1997 and references) and about 23-22 Ma (Lecca et al. 1997).

The volcanic complexes on the islands of Sant'Antioco and San Pietro, are made up of andesitic units (cupolas and domes and andesitic s. l. pyroclastites, epiclastites, and subordinately lava flows) of the late Oligocene?-early Miocene in the lower part, with 18-17 Ma K-Ar age (Maccioni et al. 1990). In the upper part there is an ignimbritic complex of the Middle Miocene made up of welded ignimbrites and ashly pomiceous pyroclastic flows of rhyolitic composition and peralkaline products of comenditic composition (16.5-15 Ma; Assorgia et al. 1990; Morra et al 1994). Finally, the Toro Rock is made up of a massive holocrystalline trachyte of 13.0 ± 0.6 Ma K-Ar age (Maccioni et al. 1990).

The andesitic complex of the island of S. Antioco lies on the Cretaceous limestones, which could belong to a Mesozoic series more or less involved in a westward thrusting on the Palaeozoic basement during the Pyrenean Orogeny (Barca and Costamagna 2000 and references). During the Neogene, this thrusting would obviously undergo an extensional tectonic inversion. Nevertheless, these structural relations should not suggest that the south-western margin of Sardinia is made up of a drowned segment of the Pyrenean, or Betic, chain, because a few samples from the margin have documented the presence of the Palaeozoic basement in the DSDP site 133-134 (Ryan et al. 1973) and in dredging D1 and D2 (Fig. 2-upper left) while in the Sea Mount Quirino (D3 of Fig. 2; Lecca 2000 and references), andesitic rocks similar to those of the Lower Miocene of the Sulcis have been dredged. At present, no important Mesozoic or Paleogenic rocks being documented, it is deduced that the margin is structured on the Hercynian basement and only sideways involved in the Pyrenean Orogeny.

A later fault system, westwards from the Sulcis Archipelago, further divided and lowered the tectonic block during different tectonic phases, which could have caused the marine transgression that started the Lower-Middle Miocene to Pliocene-Quaternary sedimentary growth of the continental shelf.

The effects of the evaporitic stage of the western Mediterranean imprinted the sedimentary pile of this shelf with a Messinian unconformity that, in the seismic profiles, is clearly recognisable below the Plio-Quaternary progradation (Lecca et al. 1986; Lecca 2000).

The seismic data and their interpretation

The seismic data available in this sector of the continental shelf of western Sardinia are mainly analogic single-channel 0.8 kJ mini-sparker lines acquired in 1981 as part of the CNR (Italian Research Council) Project "Oceanografia e Fondi Marini" (Operational Unit of the ex-Institute of Geology and Palaeontology of the University of Cagliari, Carta et al. 1986), and a few 1 kJ mini-sparker lines acquired in 1983 as part of the research study "Margini Continentali Sardi" carried out at the Department of Earth Sciences of the University of Cagliari. As regards the entire continental margin, that is from the shelf to the abyssal plain, the seismic data that have allowed to recognise structural and stratigraphic elements are the well-known Flexotir lines acquired by the OGS in Trieste (Finetti & Morelli 1973) and the R/V Charcot (Ryan et al. 1973). Moreover 10 cubic inch airgun lines were acquired subsequently by the University of Paris in collaboration with the University of Cagliari (Thomas et al. 1988-a), and single-channel analogic 1-3.5 kJ sparker lines were acquired between 1983 and 1991 as part of the above mentioned research "Margini Continentali Sardi".

Thanks to the described seismic data and to the knowledge on the nature of the rocks sampled in this area (Ryan et al. 1973; Thomas et al. 1988-b; Lecca 2000), it has been possible to recognise that the continental margin is constituted of tectonic blocks that are progressively lowered basinward (Fig.2 - bottom and Fig. 3). The largest displacements due to extensional fault zones produced the transition between the upper margin and the middle-lower margin. The main extensional fault zones that limit the various blocks caused half graben basins both at the shelf level and in the lower margin. The stratigraphic units characterising the depositional phases are easily recognised in the different structural levels of the margin. Both the basins of the shelf and those of the slope are filled with a late Oligocene-early-middle Miocene continental and marine successions. Finally, the Plio-Quaternary sequence lies upwards above the Messinian erosion truncation.

Near the studied area, the upper margin is characterised by the presence of a tectonic block, extending about NNW, of an area of about 20 x 40 km, that makes up a relatively large plateau (Fig. 2). This block, which is made up of the Palaeozoic basement, is probably overlaid by Mesozoic and Palaeogene sedimentary rocks that outcrop in the emerged areas, and finally by volcanic complexes and Miocene and Plio-Quaternary shelf sequences.

In the middle outer shelf of the studied area, above the acoustic basement, the sparker lines document the presence of two sedimentary complexes (Fig. 3). The lower complex was deposited in shelf and upper slope environments and is attributable to the Middle-Upper Miocene. It is made up of two parts separated by a clear unconformity (Fig. 3), which becomes clearer in the transition between outer and inner shelf, that is in concomitance with the outcropping of the acoustic basement (Lecca et al. 1986). The upper complex, made up mainly of falling and low stand systems tracts in an outer shelf-upper slope and attributable to several eustatic cycles of the Pliocene and Quaternary times, lies above the Messinian subaerial truncation.

The acoustic basement, which is detected in the inner shelf by the 0.8-1 kJ lines, is clearly attributable to the volcanic com-

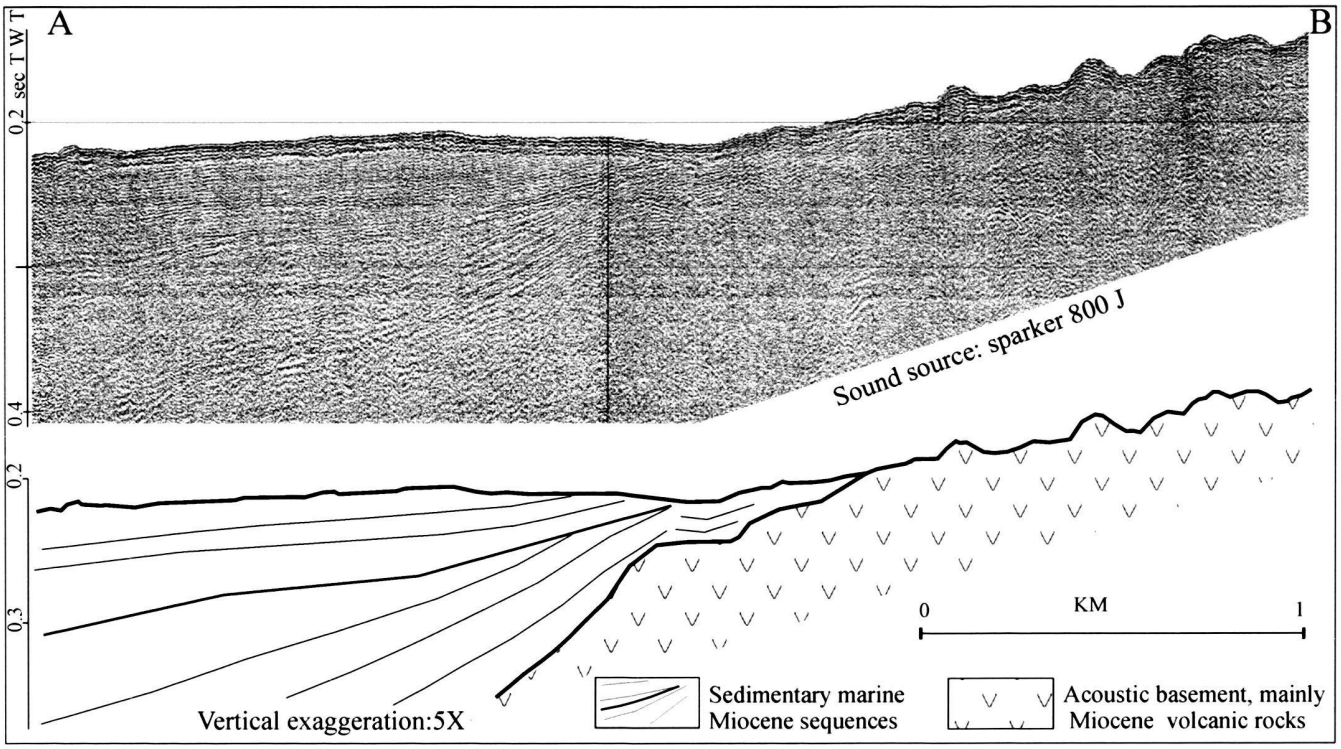

Fig. 3. Seismic reflection profile off the island of S. Pietro together with its geological interpretation. See Fig. 2 upper right for location.

plex outcropping along the western cliffs of the islands of San Pietro and Sant'Antioco. Its surface is generally shown by the attitude of the overlying stratified sediments and by its seismic facies that is generally characterised by the presence of scattered small diffraction hyperbolas and by a progressive mitigation of the seismic signal. Pattern variations of these seismic responses are present locally. They are caused by irregular variations of the seismic and therefore lithological behaviour, that are easily accounted for in a volcanic complex that shows lithologies ranging from hard and massive to stratified pyroclastic poorly competent facies. This acoustic basement outcrops in the sea bottom, it is covered by organogenic carbonate crusts, that stress its size and seismic evidence and make dredging and crabing difficult. The morphology of the sea bed is made up of the culmination of several highs (100 - 300 ms twt), a few kilometres wide and aligned parallel to the coast in a approximately north-west direction. Towards south-west the acoustic basement becomes deeper and is covered by the stratified sequence of the Miocene until it is no longer detected at about 400 - 500 ms twt (Fig. 4). The acoustic basement becomes deeper even towards north, probably due to north-east transversal faults.

Both the north-west alignment of the highs and the south-west dip suggest that the acoustic basement is controlled by a system of high-angle normal faults of north-west strike.

The entire set of data suggests that the basement is attributable to different stratigraphic levels and that it has been submitted to different erosion phases in submerged and emerged coastal environments. In fact, we can clearly recognise both an acoustic basement underlying the Miocene sequences and an acoustic basement interbedded to the Miocene sequences that could be the continuation in the inner shelf of the ignimbritic complex of the islands of San Pietro and Sant'Antioco. Near the middle shelf, the stratified sequence, which is correlated to the ignimbritic complex, could also be correlated laterally to the lower part of the Miocene marine sequence of the outer shelf.

The two kinds of basement can only be recognised when they can be correlated laterally to stratified complexes. For this reason we have reconstructed a map of isochrones of a generic acoustic basement. Therefore the acoustic basement could be the culmination of both andesitic volcanites and of the overlying ignimbritic sequence.

Aeromagnetic data

The data used for this study are part of a wide aeromagnetic survey whose data were collected in 1976 on land and offshore on Sardinia by the Compagnie Générale de Géophysique on behalf of E.M.Sa. (Ente Minerario Sardo) and Agip S.p.A. The survey was conducted in an area between 8° and 10° 30' longitude East and between 38° 40' and 41° 20' latitude North at a general constant flight altitude of 1380 m above sea level on a grid of lines and traverses oriented NE-SW and NW-SE

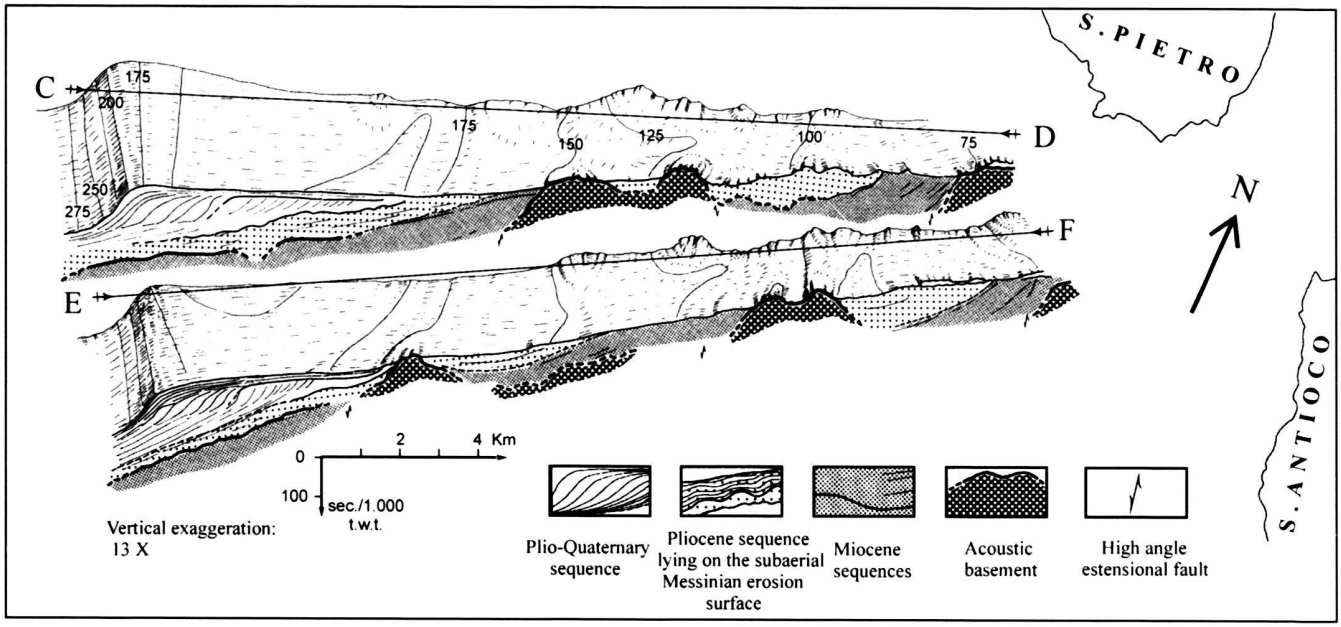

Fig. 4. Block diagrams based on the interpretation of 800 J sparker profiles, see Fig. 2 for location.

respectively. The line spacing was of 2.5 km for the NE-SW lines and of 5.0 km for the NW-SE traverses. Over the sea the spacing was enlarged to 5 km for the lines and 10 km for the traverses (Fig. 1).

The data were collected using an aircraft Cessna 402, equipped with a Caesium steam magnetometer measuring the magnetic field with an accuracy of 0.2 nT at 1 second intervals (corresponding approximately to a sampling interval of 75 m along the flight lines). The aircraft was also equipped with a LORAN C positioning system allowing the determination of the position with an accuracy of 100 m.

The effect of diurnal magnetic variations and the effects of elevation variations and instrument drift were removed from the measured data before compiling the total magnetic field map. In order to obtain a residual anomaly map a regional field with a N-S gradient of + 3.232 nT/km and + 0.726 nT/km from west to east was removed. The parameters of this field were obtained by Least Squares fitting a first order polynomial to the experimental data. In general, few magnetic anomalies with strong gradients occur in the south-western sector of the investigated area. The main feature of this magnetic pattern is an anomaly characterised by strong gradients and elongated in the WNW-ESE direction, approximately ten kilometres from the western coast of the Island of S. Antioco, near the external boundary of the western Sardinian shelf (Fig. 1).

Magnetic interpretation

A first pre-interpretation of the magnetic data was performed by means of an integrated application of the analytic signal method (Nabighian 1974; Green & Stanley 1975), the Werner deconvolution technique (Werner 1953; Hartman et al. 1971; Ku & Sharp 1983), and the Euler homogeneity equation method (Thompson 1982) along the flight line 63, 65, 67, and 69 (Fig. 1) in order to locate the position and depth of the susceptibility discontinuities. The analytic signal method and the Werner deconvolution technique are effective in cases of structures with two dimensional characters. On the other hand, the Euler homogeneity equation method does not require any assumptions concerning the geometry of the magnetic discontinuities. The three methods have the common advantage of not requiring any knowledge about the values of the susceptibility. The analytic signal method considers the source bodies as magnetically homogeneous and two-dimensional (a source body is called two-dimensional when its section can be represented by a polygon of infinite extension in the direction perpendicular to the measurement profile). The amplitude function of the analytic signal is computed by taking the square root of the sum of the squares of the horizontal and vertical derivatives of the total magnetic field $A=(\delta^2F/\delta x^2-i\delta^2F/\delta z^2)^{0.5}$. The horizontal derivative was obtained by applying a seven-point Lagrange operator to the profile data and the vertical derivative was then computed by Hilbert transforming the already computed horizontal derivative.

The amplitude of the analytic signal curve is characterised by the fact that its maxima are located directly above the anomalous contact, while the depth and slope of the contact can be deduced from two (or more) points on this curve. The latter two parameters can be obtained successfully only for well-defined anomalies that are free from interference pro-

duced by nearby anomalies. Often, the analytic signal curve is not perfectly symmetrical, indicating the presence of nearby anomalies, in which case it can only be used to indicate the position of the magnetic discontinuities along the profile. Since numerous small interfering anomalies can be recognised along the interpreted profiles, the analytic signal method has only been used to find the horizontal location of magnetic discontinuities and to give a better definition of the operators used in the Werner and Euler deconvolutions.

The Werner deconvolution method considers the anomaly to be produced by a thin dyke of infinite strike, length, and depth. The anomalous total magnetic field, expressed as a function of the distance along the measurements profile, leads to a linear equation containing four unknowns which are combinations of the following parameters: the position of the contact, its depth, its magnetic susceptibility, and its dip. Taking four points along the profile, one can derive a set of four linear equations and then solve them in order to obtain the horizontal location and the depth of the contact. Usually six or more points are used, in order to eliminate regional and end effects. A systematic application of the deconvolution operator along the profile gives a set of solutions from which the most representative can be extracted using statistical criteria and information derived from an analysis of the amplitude of the analytic signal.

The Euler deconvolution, also called the EULDPH technique (Thompson 1982), is based on Euler's homogeneity relationship. The magnetic effect of a point source can be written as a relationship between its spatial coordinates and the three derivatives of the field. In the two-dimensional case this relationship has three unknowns, which are the two co-ordinates of the source and a structural index characterising the source distribution. For the determination of the structural index the Euler deconvolution was applied with different values of it (between 0.0 and 1.0) to each profile. The value of 0.5 gave the most homogenous solutions and was therefore retained. As for the Werner deconvolution, one can systematically apply this relationship along the measured profile and obtain a set of solutions, from which the most representative can be extracted using the same criteria as for the Werner deconvolution.

The geostructural situation characterising the studied area closely fits the requirements for the application of the methods discussed above. The Werner and Euler deconvolved profiles (L63 to L69) are shown as an example in Figs. 5 and 6, each contact being marked by a different symbol.

The solutions obtained by the combination of the aforementioned methods are in quite good agreement. Along lines L65 and L69, the Werner deconvolution reveals one contact more than the Euler method, but the common solutions are situated at the same, rather shallow depth. The small differences between the solutions of the two methods can be explained by some differences in the structures of the magnetic discontinuities.

The problem of remanent magnetisation

Before starting with a detailed quantitative interpretation of magnetic anomalies, we must determine whether remanent magnetisation is to be taken into account. Because remanent magnetisation has a significant influence on the shape of the magnetic anomalies located in areas characterised by induced magnetisation, their quantitative interpretation can be biased or even erroneous if the parameters of the remanent field are not known. In order to avoid this, we decided to measure the susceptibility and the remanence of the most characteristic rocks of the continental area. The results of these determinations, together with the values of the Koenigsberg ratios $Q_m = M_r/M_i$, are listed in Table 1. These data clearly show that a remanent magnetisation exists. However, a geological analysis showed that the rocks with this magnetisation represent less than 5 percent of the total volume of the rocks taken into consideration, and therefore its influence can be regarded as negligible. Unfortunately, since most of the study area is covered by groundwater, remanence could not be measured directly on rock samples. Because remanent magnetisation can also be critical here, we had to find another way of solving the problem. For this reason, we applied the technique described by Roest & Pilkington (1993). This is based on the comparison between the horizontal gradient of the anomalies reduced to the pole (with the assumption of no remanence) and the amplitude of the two-dimensional analytic signal $A=(\delta^2F/\delta x^2 + \delta^2F/\delta y^2 - i\delta^2F/\delta z^2)^{0.5}$ of the same anomalies. If the maxima of both signals are not placed at the same location, the inducing field is not perfectly vertical as it should be after pole reduction, and therefore the remanent field will have an influence that cannot be neglected. Figs. 7-A and 7-B show the maxima of the radial horizontal derivative ($\delta F/\delta r = (\delta^2F/\delta x^2 + \delta^2F/\delta y^2)^{0.5}$) of the magnetic field reduced to the pole and the analytic signal computed from the same field. It is clear that the two pictures show the same location for both maxima (432'000/119'600) and the same orientation of the axis as the principal structure (azimuth = 42° 32' W). It can be concluded therefore that, if a remanent magnetisation exists in the area, it has a negligible influence on the inducing field. Paleomagnetic studies have also shown that, at the epoch, the trend of the magnetic field was roughly the same as the actual field.

Three dimensional analysis

To give a better representation of the susceptibility discontinuities and to take into account the three-dimensional character of the anomalies, we computed the maxima of the radial horizontal derivatives of the total field, which had already been computed. From these maxima we only retained those that presented at least two slopes in opposite directions characterising an edge in the field and consequently a magnetic discontinuity. The positions of the maxima (Fig. 8) are the most probable limits of the magnetised bodies. In order to uphold or reject this hypothesis, the magnetic discontinuities obtained from

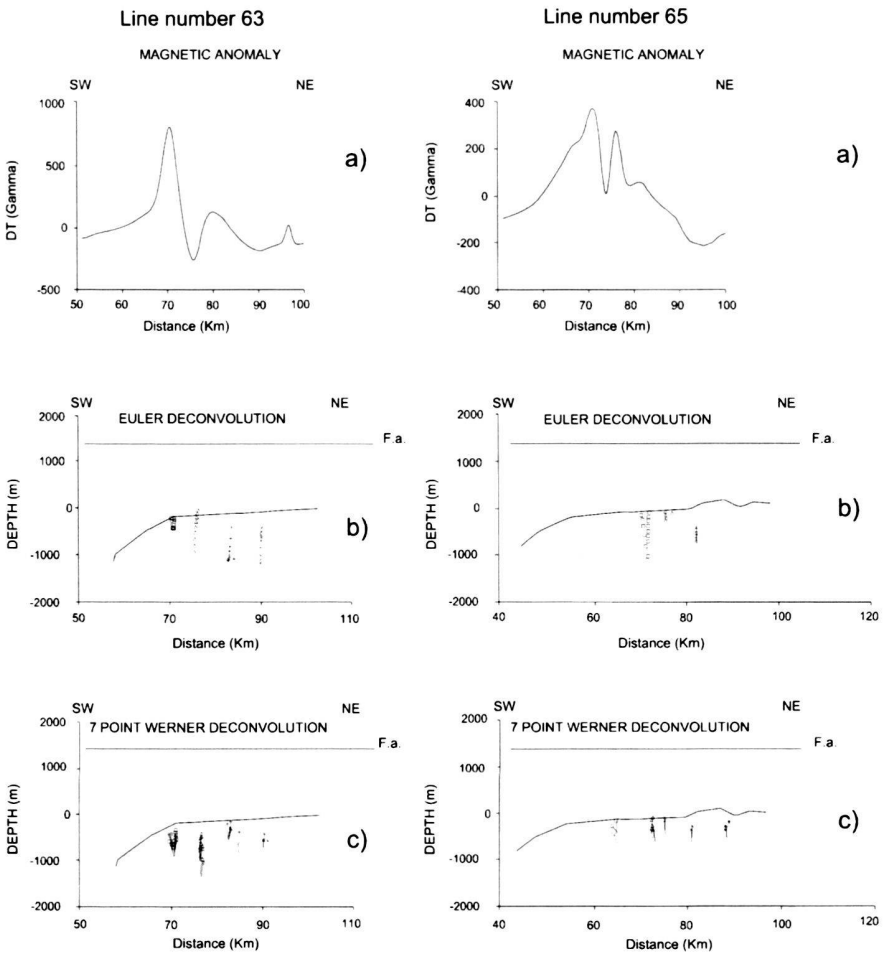

Fig. 5. Results of the Werner and Euler deconvolution of the airborne magnetic data of lines L63 and L65. The origin of the profile corresponds to that given in figure 1.

the two-dimensional deconvolution have been drawn on the same map. Though the horizontal derivative technique gives fewer solutions than the two-dimensional deconvolution, they are located in the same position. From the very good agreement between the two kinds of solutions it may be concluded that they really are the limits of the magnetic bodies.

Three-dimensional modelling

From the solutions obtained from the radial horizontal derivative technique we constructed twelve blocks delimited by straight lines passing through the lineaments in the best possible way (Fig. 9-A). The entire zone was then covered by a matrix of vertical prisms of square cross-section with a mesh size of 500 by 500 meters. A start value for the depth of the top and for the susceptibility contrast was attributed to each prism falling inside a block assuming that the effect of remanence was negligible. These start values were chosen according to the results of the two-dimensional deconvolution and with a preliminary two-dimensional magnetic modelling, not shown here. For the prisms falling outside the blocks, the depths of the top were set equal to the depth of the bottom, thus avoiding the computation. The depth of the bottom was a fixed constant at 10 km for all the prisms.

This depth corresponds to the depth after which the increase of the influence is negligible. Then the total magnetic field effect was calculated at the flight altitude on the mesh of a grid of 1 by 1 km. The result of this computation was plotted in the form of a map and compared with the experimental residual field. Using an iterative procedure the position of the corners, and the susceptibility and depth of the top of each block were adjusted until a satisfactory picture of the computed total field was obtained. For the adjustment procedure some constraints were imposed: the horizontal limits of the block were to reproduce the boundaries found by the horizontal derivative technique as well as possible, and they were to be in agreement with the geometry of the acoustic basement deduced from the high resolution reflection seismic data. A map of the result of the final computation and the experimental anomaly for comparison are shown in Figs. 10-A and 10-B. The locations of the disturbing bodies with their susceptibilities and depth is shown in Figs. 9-A and 9-B together with the depth of the acoustic basement.

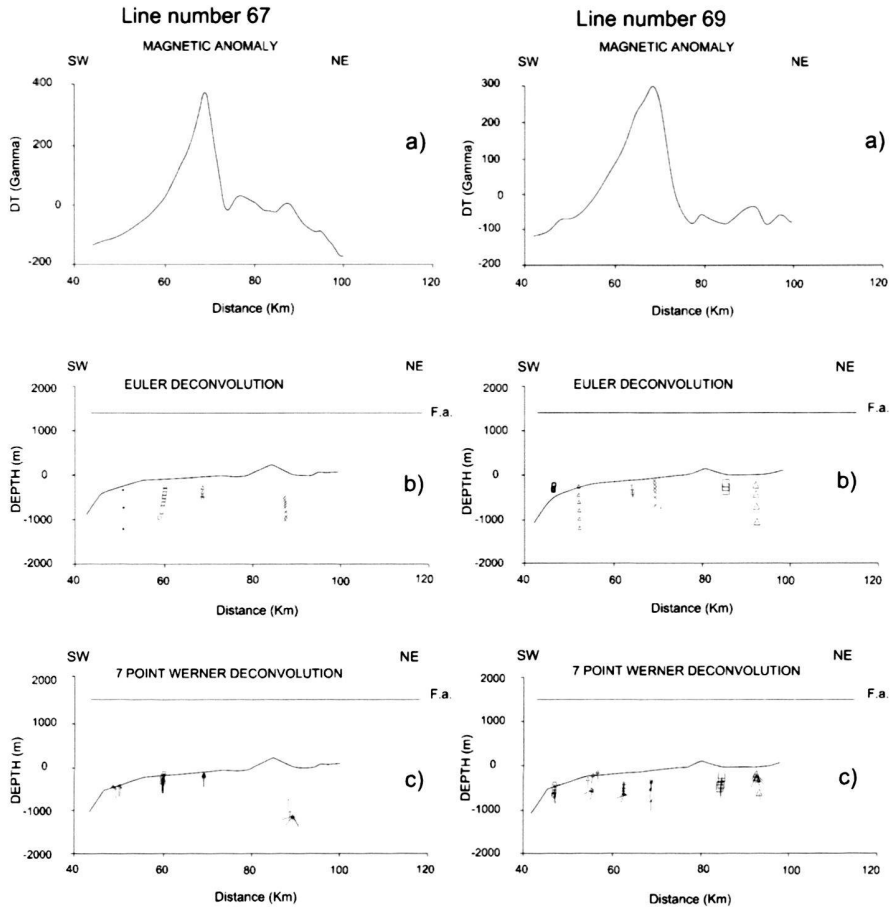

Fig. 6. Results of the Werner and Euler deconvolution of the airborne magnetic data of lines L67 and L69. The origin of the profile corresponds to that given in figure 1.

Tab. 1. Results of the determination of susceptibility and remanent magnetisation of the most typical rocks of the Sant'Antioco area. **R** is the remanent magnetisation, **K** is the susceptibility and **Q** the Koenisgberg ratio.

#	R (A/m)	K	Q	Rocks types
k01	1.43E-02	4.175e-04	**0.88**	Andesite of a volcanic dike, western Siliqua environs.
k02	5.78E-01	5.054e-02	0.29	Tonalite of a sub-volcanic stock,western Siliqua environs.
k03	2.63E-01	1.751e-02	0.37	Volcanic breccia of Gutturu de Ponti, Sulcis trough.
k04	9.93E-02	2.111e-02	0.11	Andesite inside the G. de Ponti breccia.
k05	2.10E+00	2.482e-02	**2.33**	Basaltic andesite, San Antioco (1*).
k06	4.95E-01	1.539e-02	0.71	Andesite, San Antioco (2*).
k07	2.83E+00	3.211e-02	**2.18**	Massive andesite, San Antioco (3*).
k08	3.84E-01	3.373e-02	0.25	Andesite San Antioco (2*).
k09	1.99E+00	1.158e-02	**3.33**	Ignimbrite with basal vitrophyric layer (4*).
k10	1.04E-02	1.798e-4	0.02	Cixerri sandstone.
k11	9.22E-03	2.026e-4	**1.13**	Cambro-Ordovician sandstone.

1*, 2*, 3* and 4*: lithological units 15, 19, 20 and 9 of Maccioni et al., 1990 geological map.

Discussion

The results of 3D magnetic modelling integrated with the isochrone map of the acoustic basement (Figs. 9-A and 9-B) show a clear relationship between magnetic and seismic results. Indeed, many of the magnetic contacts found by the 2D inversion techniques seem to bound magnetic bodies corresponding to a series of approximately NW trending acoustic basement highs. Analysis of the results obtained from the different inversion techniques suggests that the magnetic contacts in the south-western sector of S. Antioco are the most important in the investigated area, and can be considered as the main sources of the magnetic anomalies of this sector of the south-western Sardinian continental margin.

From the 3D magnetic interpretation two main zones with different magnetic characteristics can be identified: the northern-central zone, in the west and south sectors of the island of S. Pietro and west and north of the island of S. Antioco, both characterized by magnetic bodies with low magnetic susceptibility; and the southern zone, in the sector south-west of S. Antioco, characterized by magnetic bodies with higher magnetic susceptibility.

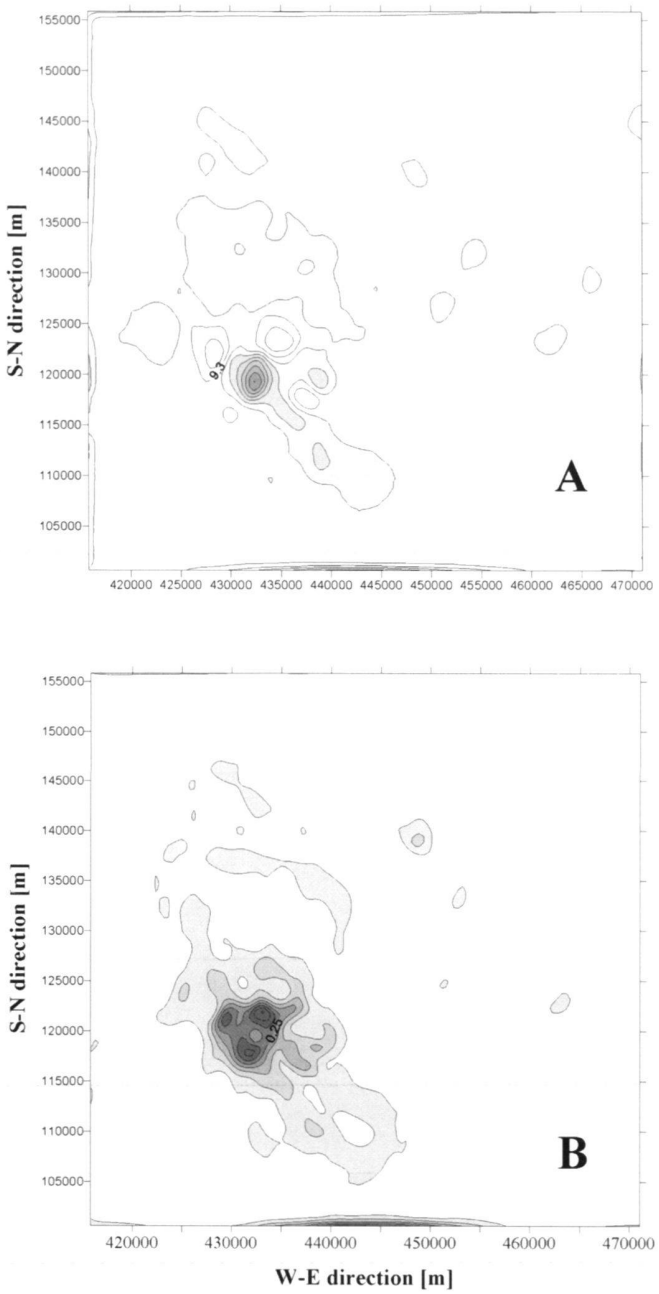

Fig. 7-A. Map of the radial horizontal derivative of the total field magnetic anomaly reduced to the pole computed without remanent magnetization, B - Map of the maximum of the analytic signal of the total field magnetic anomaly reduced to the pole computed without remanent magnetization.

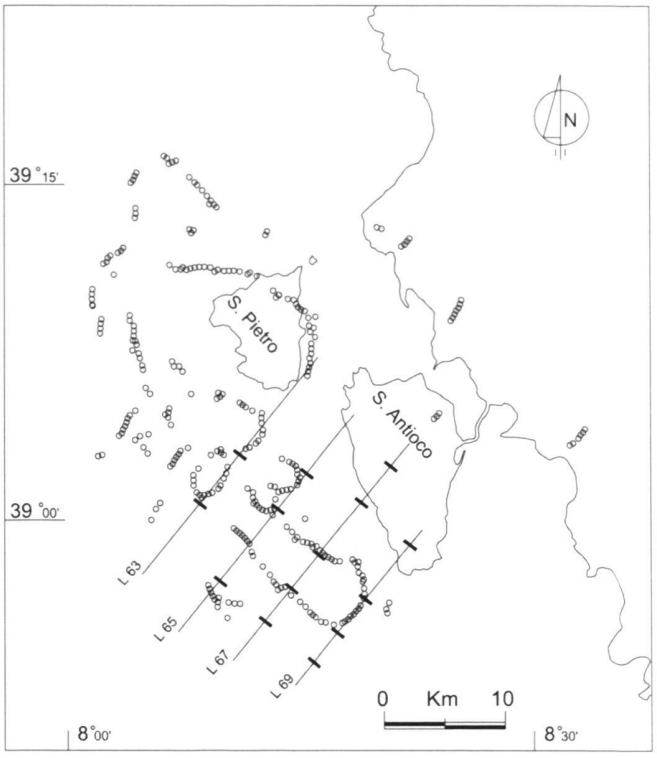

Fig. 8. Map showing the location of the maxima of the radial horizontal derivative (circles) and that of the magnetic discontinuities obtained by two dimensional Werner and Euler deconvolutions along lines L63 to L69 (bars).

It can also be observed that these highly susceptible bodies of the southern magnetic zone are deeper than the low magnetic bodies in the northern-central zone (Fig. 9-B). Moreover it was found that, in this zone, the top of the acoustic basement does not coincide with the top of the magnetic basement that gets deeper toward south-east (300 m b.s.l.) This apparent misfit can be explained by a detailed interpretation of the high-resolution seismic sparker lines. From this interpretation it is recognized that the sedimentary marine succession is made up of two sequences separated by a depositional unconformity (Fig. 4). As described above, the lower sequence is penecontemporaneous with the volcanic sequence and interlayered with volcanic units. These units are characterized by a seismic facies with a pattern of chaotic reflections and diffractions. In this particular context of transition between an emerged domain with a volcanic growth and a marine inner shelf area, different marine erosional phases developed. The erosion, probably contemporaneous with the deposition of the upper sequence, could have eroded part of the lower sequence and caused the underlying andesitic rocks to outcrop. All these events produced a heterochronous acoustic basement that can be referred to different genetic processes. Therefore, the above mentioned misfit is explained both by considering the complexity of the acoustic basement and the presence of scarcely susceptible pyroclastic and epiclastic covers that overlie the highly magnetic volcanic or sub-volcanic bodies.

Regarding the geological interpretation of the magnetic bodies that characterise the two above mentioned magnetic zones, it is clearly possible to correlate the shallower and scarcely susceptible magnetic bodies of the north-central zone

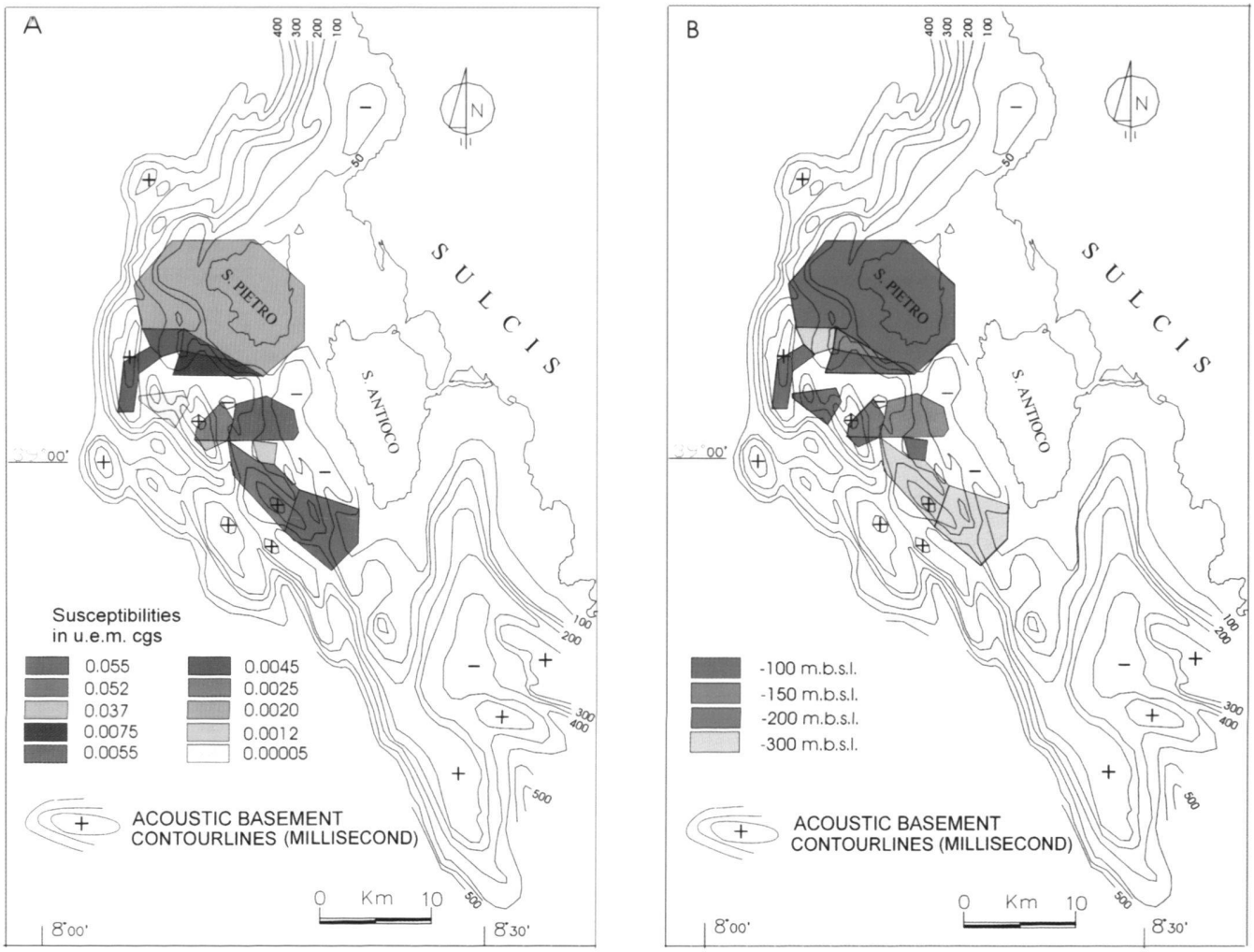

Fig. 9. Map showing the location of the magnetic blocks obtained by the three-dimensional modelling and isochrones (t.w.t.) of the acoustic basement from the high resolution reflection seismic data; A-) Susceptibility contrasts, B-) Depth of the top of the blocks.

with the low angle westward-dipping ignimbritic sequence of the island of S. Pietro. The boundaries of the above-mentioned bodies, located by the position of the magnetic solutions, can be related towards east to the fault zones that separate S. Pietro from the Sulcis block, and towards north and west to the inner sector of the continental shelf which is also fault-bounded. Towards south, the presence of smaller magnetic bodies could be due both to NNW-trending fault zones and to the irregular shape of the volcanic bodies. Therefore, in this zone, the magnetic solutions that bound the magnetic bodies follow the volcanic structure of the island of S. Pietro (cf. Garbarino et al. 1985) and can be interpreted as sub-vertical faults that mark the displacements of low-angle tabular blocks and/or volcanic contacts.

The high susceptibility magnetic bodies of the southern magnetic zone are correlable with the volcanic complexes outcropping in the southern part of the island of S. Antioco, where andesitic products of ca. 18 Ma, represented by massive bodies and scarcely stratified breccias (Maccioni et al. 1990), are present as the lowest part of the volcanic sequence. As described in the geological setting above, these volcanites lie on the Cretaceous limestones of the island of S. Antioco, which could be considered part of a Pyrenean thrusting system overlying the Hercynian basement. Therefore, in this case, the magnetic solutions could be associated to sub-vertical faults that cross the continental crust and supply sub-volcanic dikes or volcanic bodies with a high aspect ratio (Gudmundsson 1990 and references).

In this sense, the magnetic solutions bound bodies that can assume a different volcanological meaning, depending on whether they are massive lavas or fault bounded bodies. At present the elements in favour of either of the two alternatives

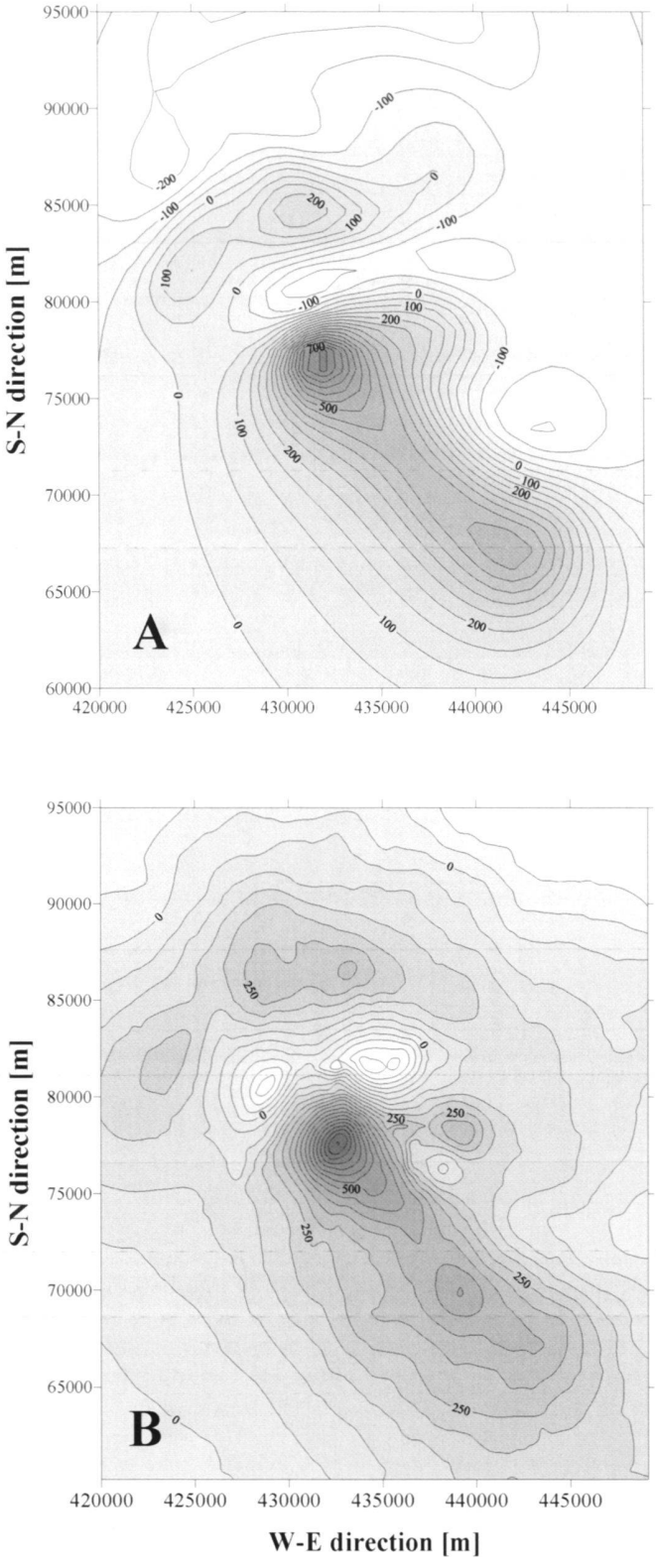

Fig. 10-A. Total field anomaly produced by the models of figures 9-A and 9-B, computed at the flight altitude, B - Experimental total field anomaly of the same area as in figure 10-A.

are not sufficient, since in both cases we have the same magnetic responses. At any rate it can generally be deduced that these contacts are correlable to the presence of a crustal fault zone that supplied the andesitic volcanism, as can be observed in other sectors of the Sardinian Rift. In fact, the andesitic volcanites are superimposed to the crustal faults, since andesitic volcanic products have poor mobility at the surface because of their own effusive behaviour.

An approximately NW trending for the above mentioned crustal faults can be deduced both from the preferential trend of the magnetic contacts and from the on-land structural features. Moreover these faults, which are located between the sub-aerial and underwater blocks of the continental margin, are evidence of extensional tectonics attributable to the early Miocene. The tectonic movements along these faults firstly activated the andesitic volcanism (late-Oligocene? – early Miocene, aged ca. 18 Ma by Maccioni et al. 1990) and later (Middle Miocene) activated the ignimbritic one. The continuation of the tectonic movements lowered the volcanic sequences of the continental margin further, causing the marine ingression during the middle-late Miocene (Fig. 11).

As regards the relationships between the study area and the Sardinian Rift, from our results we can deduce that if we consider the Rift s.l., the SW Sulcis tectonic and volcanic features can be considered part of it or framed in a late rifting phase (Barberi & Cherchi 1980; Morra et al. 1994; Lecca et al. 1997).

On the contrary, if we consider the Sardinian Rift s.s., and therefore the Rift as the only structure that propagated within the emerged Sardinia during the Oligo-Miocene, then the SW Sulcis and S. Pietro and S. Antioco sector would represent an adjoining structure that evolved more recently (ca. 18 - 15-13? Ma) than the Sardinian Rift. Moreover, based on our results, and also considering the petrochemical differences between the Sardinian Rift volcanites and the S. Pietro and S. Antioco volcanites (the latter contain peralkaline rocks: Barberi & Cherchi 1980; Morra et al. 1994), it is reasonable to consider the volcanism of the SW Sulcis block as part of the genetic and evolutionary process of the Sardinian south-western continental margin. Therefore, this tectonics could be framed in the evolution of the southern part of the Western Mediterranean basin rather than in the evolution of the Sardinian Rift system. Moreover, it should be pointed out, that from a temporal point of view in this sector the extensional movements have persisted until they become contemporaneous with the first pre-Tortonian extensional phases of the Paleo-Thyrrenian area, and more precisely in the Basins of Corsica and Sardinia, though these phases are still debatable (Rehault et al. 1987; Kasten & Mascle 1990). Therefore, a space-time transition between the end of the opening of the western Mediterranean and the beginning of the rifting of the Tyrrhenian could be inferred. Analogous interpretative hypotheses have already been presented in previous studies (Sartori 1989; Bartole et al. 1991). During this transition, extensional and/or transtensional movements would have been active contemporaneously in the two basins and subordinately inside the Sardinian Rift.

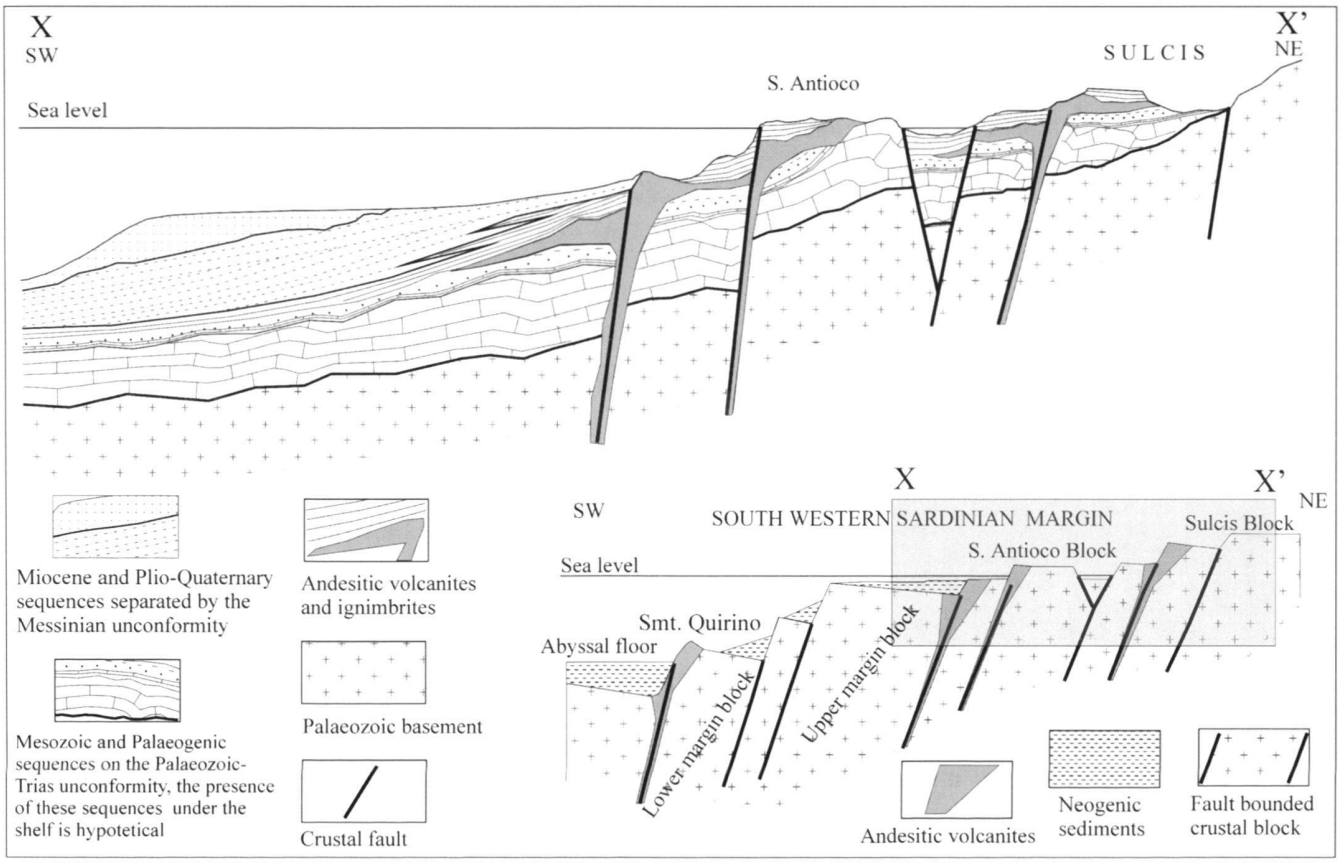

Fig. 11. Relationship between the south-west Sardinian crustal blocks and the Miocene andesitic volcanism. Not to scale cross-sections; X-X': interpretative SW-NE cross-section of the studied area.

Concluding remarks

The results presented in this paper have improved our knowledge of a submerged sector of the south-western continental margin of Sardinia. Thanks to these new elements integrated with the geological data available on nearby emerged areas, it has been possible to frame the structure of this sector in the context of the Oligo-Miocene Sardinian Rift and of the southern part of the western Mediterranean. The following is a summary of the most significant elements deduced from this study:

1) Thanks to the resolving power of the magnetic methods in the particular geological context of the upper crust of south-western Sardinia, which is essentially made up of the Hercynian basement, sedimentary covers, and andesitic volcanism, it has been possible to distinguish two different magnetic domains in the investigated area: a central-northern zone characterised by magnetic bodies with low magnetic susceptibility, and a southern zone characterised by magnetic bodies with higher magnetic susceptibility.
2) By integrating the magnetic and high resolution seismic data with the geological knowledge of the investigated area, it has been possible to correlate the central-northern zone with the presence of volcanic ignimbritic bodies and the southern zone with the presence of andesitic volcanic bodies that are believed to persist in depth.
3) The presence of an extensional fault system, which caused the lowering of the crustal blocks of the south-western upper margin during the Lower–Middle Miocene, is deduced. Futhermore it should be pointed out that the final phase (Middle-Upper Miocene) of this extensional tectonics is contemporaneous with the initial phase of the Palaeo-Thyrrenian rifting. This leads to hypothesise active extensional movements both west and east of the Sardinian-Corsican Block during pre-Tortonian times.
4) A particularly significant result of our interpretation is that the studied sector of the margin can be considered part of the genetic and evolutionary process of the southern part of the western Sardinian margin, rather than part of the evolutionary process of the s.s. Sardinian Rift, as it is generally considered.

Acknowledgements

This work was financially supported by the Italian Ministry for the University and Scientific and Technological Research (MURST - Cofin 98') and the Italian National Council of Research (CNR), (Grant # 97.00257.CT05). We thank AGIP S.p.A. for the permission to publish and E.M.Sa. (Ente Minerario Sardo) for the release of the aeromagnetic data. We also thank Mr. Giancarlo Contini for his help in figure drawing.

REFERENCES

ASSORGIA, A., FADDA, A., GIMENO TORRENTE, D., MORRA, A., OTTELLI, L. & SECCHI, F. 1990: Le successioni ignimbritiche terziarie del Sulcis (Sardegna sud-occidentale). Mem. Soc. Geol. It. 45, 951–963.

ASSORGIA, A., BROTZU, P., CALLEGARI, E., FADDA, A., LONIS, R., OTTELLI, L., RUFFINI, R., & ABRATE, T. 1992: Carta geologica del distretto vulcanico cenozoico del Sulcis. Selca, Firenze 1992.

BARCA, S. & COSTAMAGNA, L. 2000: Il Bacino paleogenico del Sulcis-Iglesiente (Sardegna SW): nuovi dati stratigrafico-strutturali per un modello geodinamico nell'ambito dell'orogenesi pirenaica. Boll.Soc.Geol It., 119, 497–515.

BARBERI, F. & CHERCHI, A. 1980: Excursion sur le Mésozoique et le Tertiaire de la Sardaigne occidentale. C.I.E.S.M. 1980, C.N.R. P.F. Geodinamica Pubbl. 345, 127 pp.

BARTOLE, R., TORELLI, L., MATTEI, G., PEIS, D. & BRANCOLINI, G. 1991: Assetto stratigrafico-strutturale del Tirreno settentrionale: stato dell'arte. Studi Geologici Camerti, Vol. Spec., 1991/1, 115–140.

BIJU DUVAL, B. & MONTADERT, L. 1977: Introduction to the structural history of the Mediterranean Basin. Int. Symp. on the struct. hist. of the Medit. Basins, Split, 1976, Technip. - Paris, 1–12.

BROTZU, P., CALLEGARI, E., MORRA, V. & RUFFINI, R. 1997: The orogenic basalt-andesite suites from the Tertiary volcanic complex of Narcao, SW-Sardinia (Italy): petrology, geochemistry and Sr-isotope characteristics. Per. Mineral. (1997), 66, 101–150.

CARTA, M., DEL FA', C., ULZEGA, A. & URAS, I. 1986: La piattaforma continentale sarda, studi geogiacimentologici, geofisici, sedimentologici e di valorizzazione dei minerali contenuti. In P.F. Oceanografia e Fondi Marini, Sottoprogetto Risorse Minerarie, Rapporto tecnico finale, CNR, Roma 1986.

CASSANO, E., MARCELLO, A., NANNINI, R., PRETTI, S., RANIERI, G., SALVADERI & R., SALVADORI, I. 1979: Rilievo aeromagnetico della Sardegna e del mare circostante. In: Ente Minerario Sardo 3, (4), 1–30.

CASSANO, E. 1990: Tyrrhenian and Western Mediterranean geomagnetic domains. Terranova, 2, 638–644.

CHERCHI, A. & MONTADERT, L. 1982: Oligo-Miocene rift of Sardinia and the early history of the Western Mediterranean Basin. Nature, 298,736–739.

DEWEY, J.F., HELMAN, M.L., TURCO, E., HUTTON, D.H.W. & KNOTT, S.D. 1989: Kinematics of the western Mediterranean. In Alpine tectonics, Coward, Dietrich & Park eds, Geol. Soc. Spec. Publ. 45, 265–283.

FAIS, S., KLINGELÉ, E.E. & LECCA, L. 1996: Oligo-miocene half graben structure in western Sardinian shelf (Western Mediterranean): reflection seismic and aeromagnetic data comparison. Marine Geology 133, 203–222.

FANUCCI, F. & MORELLI, D. 1995: Modello cinematico di evoluzione del Mediterraneo nord-occidentale. Studi Geol. Camerti, 1995/1, 383–390.

FINETTI, I. & MORELLI, C. 1973: Esplorazione geofisica dell'area circostante il blocco sardo-corso. Rend. Sem. Fac. Sc. Univ. Cagliari, Suppl. 43, 213–238.

GARBARINO, C., MACCIONI, L., & SALVADORI, I. 1985: Carta geopetrografica dell'Isola di S.Pietro (Sardegna). Scala 1:25.000, Selca, Firenze.

GREEN, R. & STANLEY, J.M. 1975: Application of a Hilbert transform method to the interpretation of surface-vehicle magnetic data. Geophys. Prospect. 23, 18–27.

GUDMUNDSSON, A. 1990: Emplacement of dikes, sills and crustal magma chambers at divergent plate boundaries. Tectonophysics 176, 257–275.

HARTMAN, R.R., TESKEY, D.J. & FRIEDBERG, J. 1971: A system for rapid digital aeromagnetic interpretation. Geophysics 36, 891–918.

KASTEN, K. & MASCLE, J. 1990: The geological evolution of the Tyrrhenian Sea: an introduction to the scientific results of ODP LEG 107. Proceedings of the ODP, Scientific Results, vol. 107, 3–26.

KU, C.C. & SHARP, J.A. 1983: Werner deconvolution automated magnetic interpretation and its refinement using Marquardt's inverse modeling. Geophysics 48, 754–774.

LECCA, L., CARBONI, S., SCARTEDDU, R., SECHI, F., TILOCCA, G. & PISANO, S. 1986: Schema stratigrafico della piattaforma continentale occidentale e meridionale della Sardegna. Mem. Soc. Geol. It. 36, 31–40.

LECCA, L., LONIS, R., LUXORO, S., MELIS, E., SECHI, F. & BROTZU, P. 1997: Oligo-Miocene volcanic sequences and rifting stages in Sardinia: a riview. Periodico di Mineralogia, 66, 7–61, 1carta., Roma, 1997.

LECCA, L. 2000: La piattaforma continentale miocenico-quaternaria del margine occidentale sardo: blocco diagramma sezionato. Rend. Sem. Fac. Sc. Univ. Cagliari 1, (70). Cagliari 2000, in press.

MACCIONI, L., MARCHI, M. & ASSORGIA, A. 1990: Carta geopetrografica dell'Isola di S.Antioco (Sardegna sud-occidentale). Scala 1:25.000, Selca, Firenze.

MATTEUCCI, R., 1985: Marine Eocene of Sardinia. In 19th European Micropaleontological Colloquium Guidebook, A.Cherchi Ed., Cagliari, 80–86.

MORRA, V., SECHI, F. & ASSORGIA, A. 1994: Petrogenetic significance of peralkaline rocks from cenozoic calcalkaline volcanism from SW Sardinia (Italy). Chem. Geol. 118,109–142

NABIGIAN, M.N. 1974: Additional comments on the analytic signal of two-dimensional magnetic bodies with polygonal cross-section. Geophysics 39, (1), 85–92.

PECORINI, G. & POMESANO-CHERCHI, A. 1969: Ricerche geologiche biostratigrafiche sul Campidano meridionale (Sardegna). Mem. Soc. Geol. It. 8, 421–451.

REHAULT, J.P., BOILLOT, G. & MAUFRET, A. 1985: The western Mediterranean Basin. In Geological evolution of the Mediterranean Basin, D.J Stanley & F.C.Wezel eds., Springer-Verlag, 101–129.

REHAULT, J.P., MOUSSAT, E. & FABBRI, A. 1987: Structural evolution of the Tyrrhenian back-arc basin. Marine Geology 74, 123–150.

RYAN, W.B.F., HSÜ, K.J., CITA, M.B., DUMITRICA, P., LORT, J., MAYNC, W., NESTEROFF, W.D., PAUTOT, G., STRADNER, H. & WEZEL, C.F. 1973: Boundary of Sardinia slope with Balearic abyssal plain-sites 133 and 134. Init. Rep. D.S.D.P. vol. 13, pt.1, U.S.G.P.O., 465–514.

ROEST, W.R. & PILKINGTON, M. 1993: Identifying remanent magnetization effects in magnetic data. Geophysics 58, 5, 653–659.

SARTORI, R. 1989: Evoluzione neogenico-recente del bacino tirrenico e suoi rapporti con la geologia delle aree circostanti. Giornale di Geologia, ser.3°, vol. 51/2, 1–39.

THOMAS, B., LECCA, L. & GENNESSEAUX, M. 1988a: Structuration et morphogenese de la marge occidentale de la Sardaigne au Cénozoique. C.R. Acad. Sci. Paris, t. 306, Série II,: 903–910.

THOMAS, B., GENNESSEAUX, M. & LECCA, L., 1988b: La structure de la marge occidentale de la Sardaigne et la fragmentation de l'ile au cenozoique. Mar. Geol. 83, 31–41.

THOMPSON, D.T. 1982: Euldph: A new technique for making computer-assisted depth estimates from magnetic data. Geophysics 47, 31–37.

WERNER, S., 1953: Interpretation of magnetic anomalies as sheet-like bodies. Serv. Geol. Unders., Ser. C, Arsb. 43, 06.

ZANOLLA, C., MORELLI, C. & MARSON, I. 1998: The magnetic anomalies of the Mediterranean Sea (IBCM-M). Boll. Geof. Teor. Appl. 39, (1), 1–36.

Manuscript received February 20, 2001
Revision accepted April 20, 2002